EEG DENOISING USING WAVELET ENHANCED ICA

by

Md Danish Jamil,

M.Tech, signal processing and digital design,
Delhi Technological University, Delhi, 2015

SUBMITTED TO THE DEPARTMENT OF ELECTRONICS & COMMUNICATION ENGG,
IN PARTIAL FULFILLMENT OF THE REQUIREMENTS FOR THE DEGREE OF

MASTER OF TECHNOLOGY IN SIGNAL PROCESSING AND DIGITAL DESIGN

AT

DELHI TECHNOLOGICAL UNIVERSITY, DELHI

JUNE 2015

Under the Supervision of

MR. M.S. CHOUDHARY,
Associate Professor,
Department of Electronics & Communication Engineering,
Delhi Technological University,
Delhi, India.

DEPARTMENT OF ELECTRONICS AND COMMUNICATION ENGINEERING
Delhi Technological University,
(*formerly* Delhi College of Engineering)
Bawana Road, Delhi – 110042

Dedicated to my Parents, Mentor, Friends

and

the Almighty…

Table of Contents

Chapter 1 : Introduction

In human brain neural activities start at 17th -23rd month of prenatal development stage, since then throughout life our brain generates electrical signal known as electroencephalogram(EEG) , and it not only represents the brain activity but also the activity of rest part of our body. As we can analyse our body's behaviour by analysing EEG signals, this motivates us to deep analysis of EEG signals.

1.1 Electroencephalography (EEG)

EEG is an electrical signals which can be measured from our scalp using electrodes. It is very popular now a days, because it is one of the means for brain computer interface.

1. History:-

In early 19th century EEG signal was first registered by Carlo Matteucci and Emil Du Bois-Reymond and they said it is an electrical signal generated by our brain and then onwards the study of neuro physiology started[1,2].

The first person to find the existence of EEG signal was Hans Berger in 1920, he recorded the first EEG signal of human on photographic paper for up to three minutes in 1929. To record this signal only a one channel bipolar method was used with fronto-occipital leads. The first recording of EEG signal had the main component as alpha rhythm and the alpha blocking response.

The first biological amplifier for the measurement of brain electrical signals was devised in early 20th century by Toennies from Berlin designed. The Rockefeller foundation designed a differential amplifier for EEG measurement. Multichannel recordings and use of large number of electrodes to study complete brain region was demonstrated by Kornmuller [3]. For the first time EEG work for epileptic manifestation and demonstration of epileptic spikes were presented by Fischer and Lowenbach [4-6].

2. Neural Activities

The central neural system generally comprises of nerve cells and glia cells. These cells are located between the neurons. A nerve cell can be further divided into three parts i.e. Axons, dendrites, and cell bodies. Response to stimuli and transmission of information over long distance are done by nerve cells. A nerve cell body consists of a single nucleus and contains most of the nerve cell

metabolism. Synthesis of proteins occur in the cell body, and are conveyed to other parts of the nerve. An axon is of barrel shape and can have several meters length in vertebrates, and its major function is to transmit an electrical impulse .The length of axon generally ranges from a fraction of a millimeter to more than a meter in humans. There exist an axonal transport system which has 'molecular motors', which ride upon tubulin rails and delivers proteins to the ends of the cells.

Dendrites are connected to the axons or dendrites of other cells and their function is to transmit the signal or receive the signal from other nerves. All nerves are connected to almost 10,000 other nerves, through dendritic connections in brain.

The junctions (called synapses) of axons and dendrites, or dendrites and dendrites of other cells are sites for synaptic currents which are mainly responsible for activities inside the CNS. The membrane of the cell body has a negative potential of 60–70 mV Variations in synaptic activity leads to change in this potential. If an action potential travels along the fiber, which ends in an excitatory synapse, an excitatory postsynaptic potential (EPSP) occurs in the following neuron. A summation of EPSPs would occur, if two action potentials travel along the same fiber over a short distance, which will produce an action potential on the postsynaptic neuron, providing a certain threshold of membrane potential is reached. Hyperpolarization occurs, if the fiber ends in an inhibitory synapse, and this indicates an inhibitory postsynaptic potential [8, 9]. A schematic diagram of the above discussed activities is shown in fig 1.1.

The generation of an IPSP leads to either overflow of cations from the nerve cell or an inflow of anions into the nerve cell .This results in change in change in potential along the nerve cell membrane. Within the intra- and extracellular space, primary transmembranous currents generates secondary inonal currents along the cell membranes. Generation of field potentials is resulted with the flow of these currents through extracellular space. These field potentials, usually with less than 100 Hz frequency, are called EEGs when there are no changes in the signal average and DC if there are slow drifts in the average signals, which may mask the actual EEG signals. . A combination of EEG and DC potentials is often observed for some abnormalities in the brain such as seizure (induced by pentylenetetrazol), hypercapnia, and asphyxia [10].

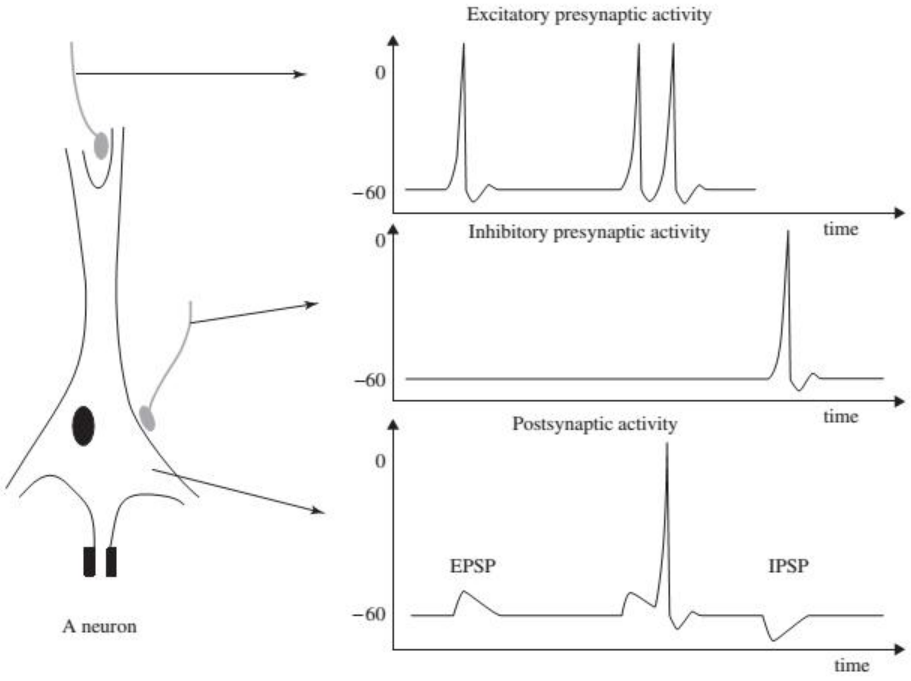

Figure 1.1 The neuron membrane potential changes and current flow during synaptic activation recorded by means of intracellular microelectrodes.

3. EEG Generation

An EEG signal is a measurement of currents that flow during synaptic excitations of the dendrites of many pyramidal neurons in the cerebral cortex. Production of synaptic currents takes place within the dendrites when the brain cells (neurons) are activated. This current generates a magnetic field measurable by electromyogram (EMG) machines and a secondary electrical field over the scalp measurable by EEG systems.

Differences of electrical potentials are caused by summed postsynaptic graded potentials from pyramidal cells that create electrical dipoles between the soma (body of a neuron) and apical dendrites, which branch from neurons (Figure 1.2). The current in the brain is generated mostly by pumping the positive ions of sodium, Na + , potassium, K + , calcium, Ca++, and the negative ion of chlorine, Cl−, through the neuron membranes in the direction governed by the membrane potential [7].

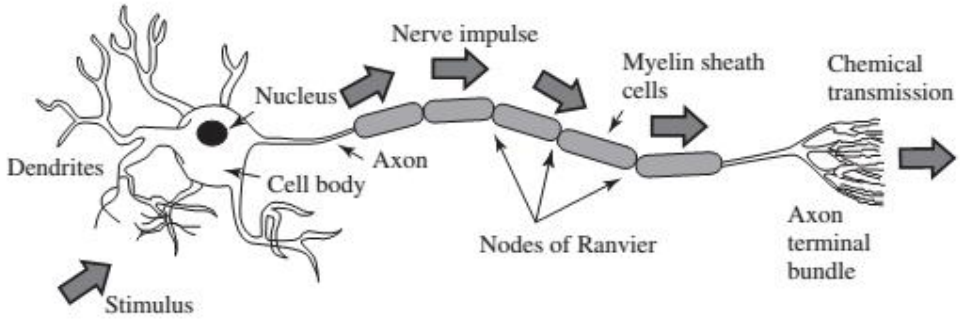

Figure: 1.2 neuron's structure

The different layers of human head consists of the scalp, skull and brain (Figure 1.3). In between, many other thin layers are there. The skull attenuates the signals approximately one hundred times more than the soft tissue. Generation of noise takes place either within the brain (internal noise) or over the scalp (system noise or external noise). Therefore, only large populations of active neurons can generate enough potential to be recordable using the scalp electrodes. Amplification of these signals are later on done for display.

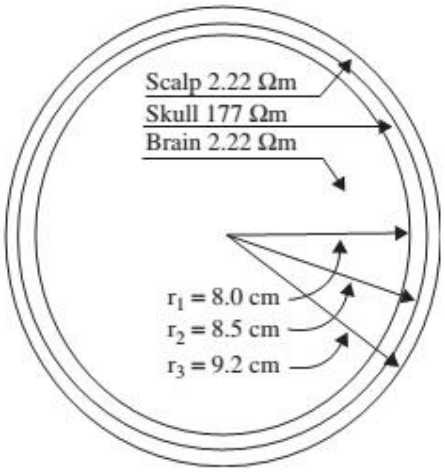

Figure: 1.3 three main layers of brain, their resistivity and thickness

During the time of birth when the CNS becomes complete and functional, approx. 10^{11} neurons are developed [11]. This makes an average of 10 4 neurons per cubic mm. Neurons are interconnected into neural nets through synapses. Approximately 5×10 14 synapses exists in adults. The number of synapses per neuron increases with age, whereas the number of neurons decreases with age.

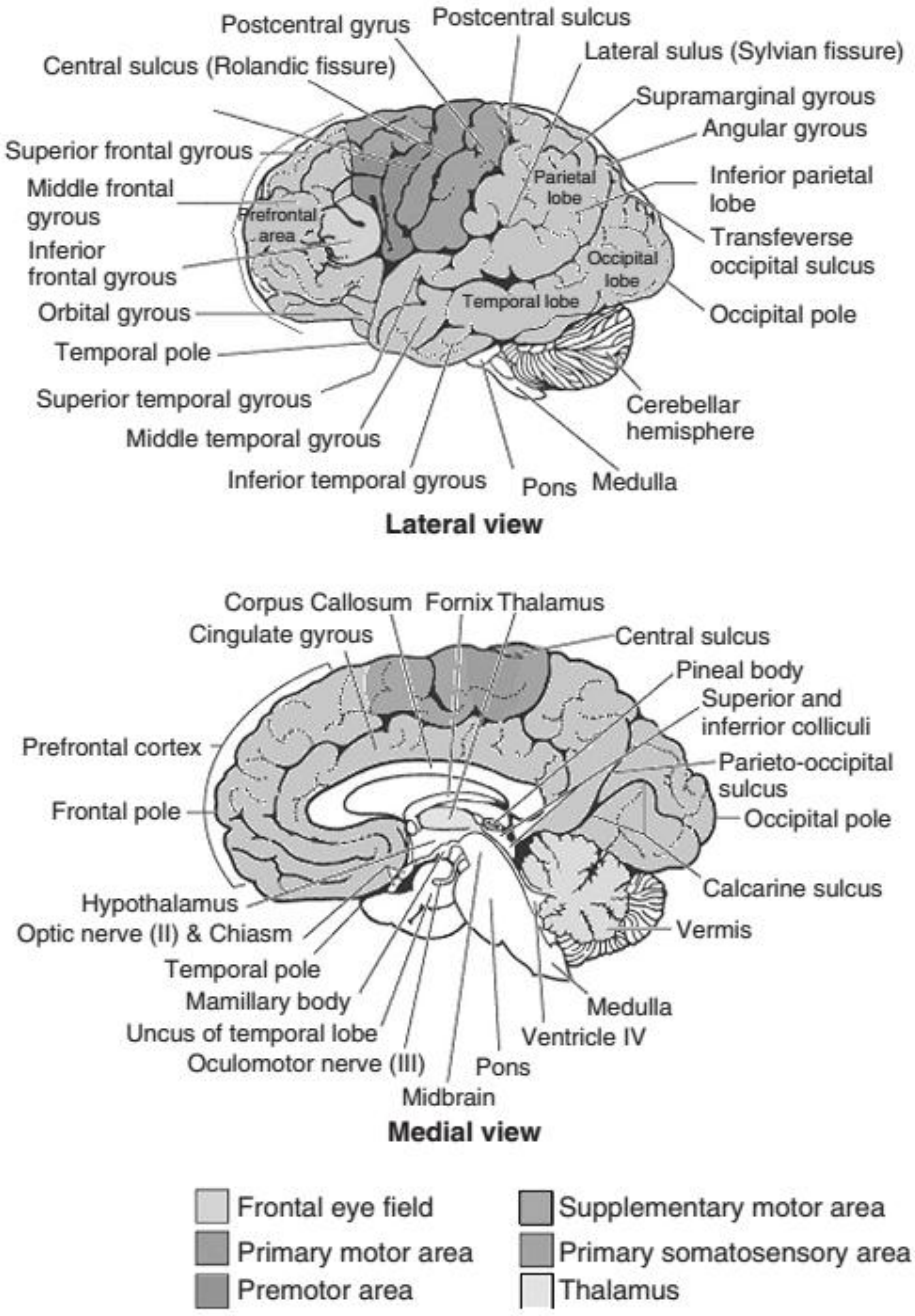

Figure: 1.4 major parts of brain representation

From an anatomical point of view, the brain consists of three major parts i.e. the cerebrum, cerebellum, and brain stem (Figure 1.4). The cerebrum consists of both left and right lobes of the brain with highly convoluted surface layers called the cerebral cortex. The region of movement initiation, conscious awareness of sensation complex analysis, and expression of emotions and behavior are taken care of by cerebrum. The coordination of voluntary movements of muscles

and maintaining balance are the functions of cerebellum. Involuntary functions such as respiration, heart regulation, biorhythms, and neuro hormone and hormone sections are controlled by the brain stem [12].

Based on the above section it is clear that the study of EEGs paves the way for diagnosis of many neurological disorders and other abnormalities in the human body. The acquired EEG signals from a human (and also from animals) may, for example, be used for investigation of the following clinical problems [12, 13]:

(a) Monitoring alertness, coma, and brain death;

(b) Locating areas of damage following head injury, stroke, and tumour;

(c) Testing afferent pathways (by evoked potentials);

(d) Monitoring cognitive engagement (alpha rhythm);

(e) Producing biofeedback situations;

(f) Controlling anaesthesia depth (servo anaesthesia);

(g) Investigating epilepsy and locating seizure origin;

(h) Testing epilepsy drug effects;

(i) Assisting in experimental cortical excision of epileptic focus;

(j) Monitoring the brain development;

(k) Testing drugs for convulsive effects;

(l) Investigating sleep disorders and physiology;

(m) Investigating mental disorders;

(n) Providing a hybrid data recording system together with other imaging modalities.

The rich potential for EEG analysis motivates the need for advanced signal processing techniques to aid the clinician in their interpretation.

4. Brain Rhythms

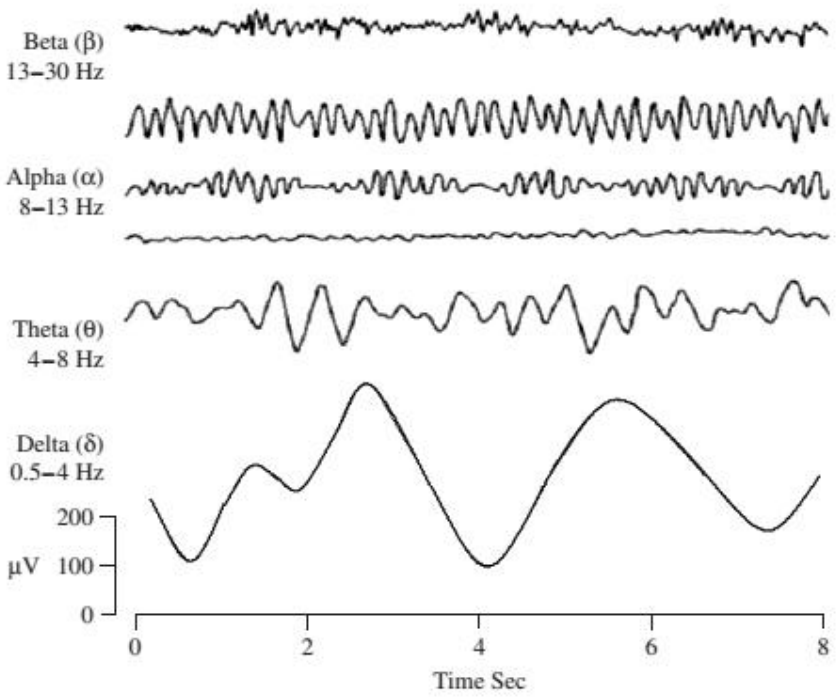

Figure: 1.5 the main four rhythm found in EEG signals.

Visual inspection of EEG signals helps in diagnosis of many brain disorders. Variations in amplitudes and frequencies of such signals change happens from one state of a human to another, such as wakefulness and sleep in healthy humans. Changes in the characteristics of the wave happens with age. Based on the different frequency ranges, the brain waves can be subdivided into five major types i.e. alpha (α), theta (θ), beta (β), delta (δ), and gamma (γ). In 1929, Berger introduced the existence of alpha and beta waves. Jasper and Andrews (1938) introduced the gamma waves (above 30 Hz). The delta rhythm was introduced by Walter (1936) to designate all frequencies below the alpha range. Those waves having frequencies within the range of 4–7.5 Hz were known as theta waves and were introduced by Wolter and Dovey in 1944 [14].

Delta waves lie within the range of 0.5–4 Hz and are primarily associated with deep sleep and may be present in the waking state. Artefact signals caused by the large muscles of the neck and jaw are confused with the genuine delta response. This is because the muscles are near the surface of the skin and produce large signals, whereas the signal that is of interest originates from deep within the brain and is severely attenuated in passing through the skull.

Theta waves lie within the range of 4–7.5 Hz and have been associated with access to unconscious material, creative inspiration and deep meditation. It is known that healers and experienced mediators have an alpha wave that gradually lowers in frequency over long periods of time. The theta waves are dominant in infants and children. Larger contingents of theta wave activity in the waking adult are abnormal and are caused by various pathological problems. The changes in the rhythm of theta waves are examined for maturational and emotional studies [15].

Most subjects produce some alpha waves with their eyes closed, that is why it is claimed that it is a waiting or scanning pattern produced by the visual regions of the brain. By opening the eyes, by hearing unfamiliar sounds, by anxiety, or mental concentration or attention, it can be reduced or eliminated.

While remaining in the alpha state, Albert Einstein could solve complex mathematical problems, although generally beta and theta waves are also present. An alpha has an amplitude of normally less than 50μV, which is a higher amplitude compared to the occipital areas. The origin and physiological significance of an alpha wave is still unknown and yet more research has to be undertaken to understand how this phenomenon originates from cortical cells [16].

The electrical activity of the brain is the beta wave which varies within the range 14-26 Hz (though in some literature no upper bound is given). The usual waking rhythm of the brain associated with active thinking, active attention, focus on the outside world, or solving concrete problems, is a beta wave, and is found in normal adults. When a human is in a panic state, a high-level beta wave may be acquired. Chiefly over the frontal and central regions, rhythmical beta activity is encountered. A central beta rhythm and the rolandic mu rhythm are related and are blocked by motor activity or tactile stimulation. Normally, the amplitude of beta rhythm is under 30μV. The beta wave may also be enhanced because of abone defect and also around tumoural regions, similar to the mu rhythms. The frequencies above 30 Hz (mainly up to 45 Hz) correspond to the gamma range (sometimes called the fast beta wave). The occurance of these rhythms are very rare. For confirmation of certain brain diseases, detection of these rhythms are used. In the frontocentral area, the regions of high EEG frequencies and highest levels of cerebral blood flow (as well as oxygen and glucose uptake) are located. For event-related synchronization (ERS) of the brain, the gamma wave has been proven a good indication and to demonstrate the locus for right and left index finger movement, right toes, and the rather broad and bilateral area for tongue movement, it can be used.

Mostly in the range of 200–300 Hz, Waves in frequencies much higher than the normal activity range of EEG have been found in cerebellar structures of animals but in clinical neurophysiology, they have not played any role. The typical normal brain rhythms with their usual amplitude levels have been shown in fig 1.5.

The projection of neural activities that are attenuated by leptomeninges, cerebrospinal fluid, dura matter, bone, galea, and the scalp are EEG signal in general. Amplitudes of 0.5–1.5 mV has been shown by Cartographic discharges and up to several millivolts for spikes. However, the amplitudes commonly lie within 10–100μV on the scalp. If the state of the subject does not change the above rhythms may last, and therefore they are approximately cyclic in nature. On the other hand, there are other brain waveforms, which may:

The delta wave is observed in infants and sleeping adults, the theta wave in children and sleeping adults, the alpha wave is detected in the occipital brain region when there is no attention, and the beta wave appears frontally and parietally with low amplitude.

(a) Have a wide frequency range or appear as spiky-type signals, such as K-complexes, vertex waves (which happen during sleep), or an alpha-type rhythm due to a cranial bone defect [35], called a breach rhythm, which is, mainly found over the mid-temporal region (under electrodes T3 or T4), and some seizure signals and does not respond to movement.
(b) Be a transient such as an event-related potential (ERP) and contain positive occipital sharp transient (POST) signals (also called rho (ρ) waves).
(c) Originated from the defective regions of the brain such as tumoural brain lesions.
(d) Be spatially localized and considered as cyclic in nature, but can be easily blocked by physical movement such as mu rhythms. Mu represents motor and is strongly related to the motor cortex. In terms of amplitude and frequency, Rolandic (central) mu is related to posterior alpha. The topography and physiological significance are quite different, however. Functioning and the changes in brain (mostly bilateral) activities subject to physical and imaginary movements can be investigated, from the mu rhythm the cortical. The mu rhythm has also been used in feedback training for several purposes such as treatment of epileptic seizure disorder [14].

5. EEG Recording and Measurement

For early diagnosis of a variety of diseases, acquiring signals and images from the human body has become important. Such data can be in the form of electrobiological signals such as an electrocardiogram (ECG) from the heart, electromyogram (EMG) from muscles,

electroencephalogram (EEG) from the brain, magnetoencephalogram (MEG) from the brain, electrogastrogram (EGG) from the stomach, and electroocclugram (or electrooptigram, EOG)from eye nerves.

Either EEG, MEG, or fMRI may be used to register the functional and physiological changes of our brain. However, in comparison with EEG and MEG, the application of fMRI is very limited due to a number of important reasons.

A. The time resolution of fMRI image sequences is very low (for example approximately two frames/s), whereas using EEG or MEG signals, the complete EEG bandwidth can be viewed
B. Using fMRI, many types of mental activities, brain disorders, and malfunctions of the brain cannot be registered since on the level of oxygenated blood, their effect is low.
C. The accessibility to fMRI (and currently to MEG) systems is restricted and costly.
D. However, the spatial resolution of EEG, is limited to the number of recording electrodes (or number of coils for MEG).

Using simple galvanometers, the first electrical neural activities were registered. A mirror was used to reflect the light projected to the galvanometer on the wall, in order to magnify the fine variation of the pointer. In the d'Arsonval galvanometer, later, contained the mirror placed on a movable coil and the when a current passed the coil light focused on the mirror was reflected. Later, by Lippmann and Marey [17], the capillary electrometer was introduced. In 1903, by Einthoven a very sensitive and more accurate measuring instrument was invented, known as the string galvanometer. It enabled photographic recording and became the standard instrument for a few decades. More recent EEG systems consist of a number of delicate electrodes, a set of differential amplifiers (one for each channel) followed by filters [12], and needle (pen)-type registers. On plain paper or paper with a grid, the multichannel EEGs could be plotted. After this instrument was introduced to the market, researchers tried to come up with a computerized system, which could digitize and store the signals. It was soon understood that the signals must be in digital form, to analyze EEG signals. For this, sampling, quantization, and encoding of the signals was required. As the number of electrodes grows the data volume, in terms of the number of bits, increases. The newly invented, computerized systems allowed variable settings, stimulations, and sampling frequency, and some are prepared with simple or advanced signal processing tools for signal processing.

The analogue is converted to digital EEG by a multichannel analogue-to-digital converters (ADCs). Fortunately, the effective bandwidth for EEG signals is limited to approximately 100 Hz. This bandwidth may be considered to be even half of this value, for this application. Therefore, it is often enough for sampling the EEG signals, with a minimum frequency of 200 samples/s (to satisfy the Nyquist criterion). Sampling frequencies of up to 2000 sample/s may be used in some applications where for representation of brain activities in frequency domain, a higher resolution is required. The quantization of EEG signals is normally very fine in order to maintain the diagnostic information. Each signal sample is represented upto 16 bits which is very popular for the EEG recording system. For archiving the signals massive, especially for sleep EEG and epileptic seizure monitoring records, this makes the necessary memory volume. However, in general, the memory size for archiving the radiological images is often much larger than that used for archiving the EEG signals.

A simple calculation shows that for a one hour recording from 128-electrode EEG signals sampled at 500 samples/s a memory size of $128\times60\times60\times500\times16\approx3.68$ Gbits ≈0.45 Gbyte is required. There should be enough storage facilities such as in today's technology Zip disks, CDs, large removable hard drives, and optical disks for longer recordings of a large number of patients. Although the format of reading the EEG data for different EEG machines may differ, these formats are easily convertible to spreadsheets readable by most signal processing software packages such as MATLAB.

For acquiring high quality data, the EEG recording electrodes and their proper function are crucial. Different types of electrodes are often used in the EEG recording systems, such as:

- disposable (gel-less, and pre-gelled types);
- reusable disc electrodes (gold, silver, stainless steel, or tin);
- headbands and electrode caps;
- saline-based electrodes;
- Needle electrodes.

Electrode caps are often used for multichannel recordings with a large number of electrodes. Commonly used scalp electrodes consist of Ag–AgCl disks which is less than 3 mm in diameter, with long flexible leads that can be plugged into an amplifier. Under the skull with minimal invasive operations, needle electrode have to be implanted. High impedance between the cortex

and the electrodes as well as the electrodes with high impedances can lead to distortion, which can even mask the actual EEG signals. The electrode impedances should read less than 5k and be balanced to within 1k of each other to enable a satisfactory recording. The impedances are checked after each trial, for more accurate measurement. Distribution of the potentials over the scalp (or cortex) is not uniform [18] due to the layered and spiral structure of the brain.

6. Conventional Electrode Positioning

The International Federation of Societies for Electroencephalography and Clinical Neurophysiology has recommended the conventional electrode setting (also called 10–20) for 21 electrodes (excluding the earlobe electrodes), as depicted in Figure 1.6 [17]. Often the earlobe electrode A1 connected to the left earlobe and the earlobe electrode A2 connected to the right electrode are used as the reference electrodes. The 10–20 system avoids both eyeball placement and considers some constant distances by using specific anatomic landmarks from which the measurement would be made and then uses 10 or 20 % of that specified distance as the electrode interval. The odd and even electrodes are on the left and right respectively. The rest of the electrodes are placed in between the above electrodes equidistance between them, for setting a larger number of electrodes using the above conventional system. For example, C1is placed between C3and Cz.

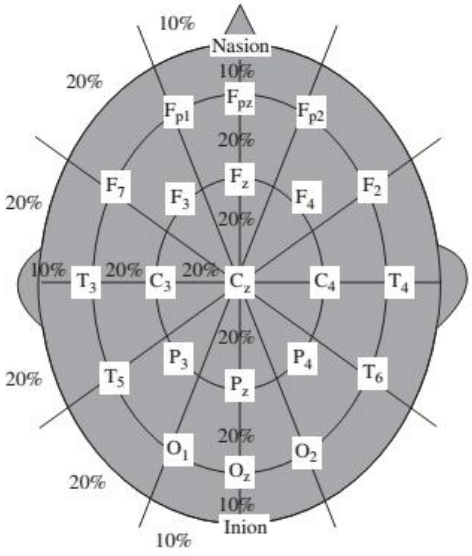

Figure: 1.6 Conventional 10–20 EEG electrode positions

For the measurement of EOG, ECG, and EMG of the eyelid and eye surrounding muscles, extra electrodes are sometimes used. A single channel may be used, in some applications such as ERP

analysis and brain computer interfacing. The position of the corresponding electrode has to be well determined.

1.2 Conditioning the Signals

The raw EEG signals have amplitudes of the order of μvolts and contain frequency components of up to 300 Hz. The signals have to be amplified before the ADC and filtered, either before or after the ADC in order to reduce the noise and make the signals suitable for processing and visualization to retain the effective information. The filters are designed in such a way so that it does not introduce any change or distortion to the signals. To remove the disturbing very low frequency components such as those of breathing, high pass filters with a cut-off frequency of usually less than 0.5 Hz are used. By using low pass filters with a cut-off, frequency of approximately 50–70 Hz, high-frequency noise is mitigated.

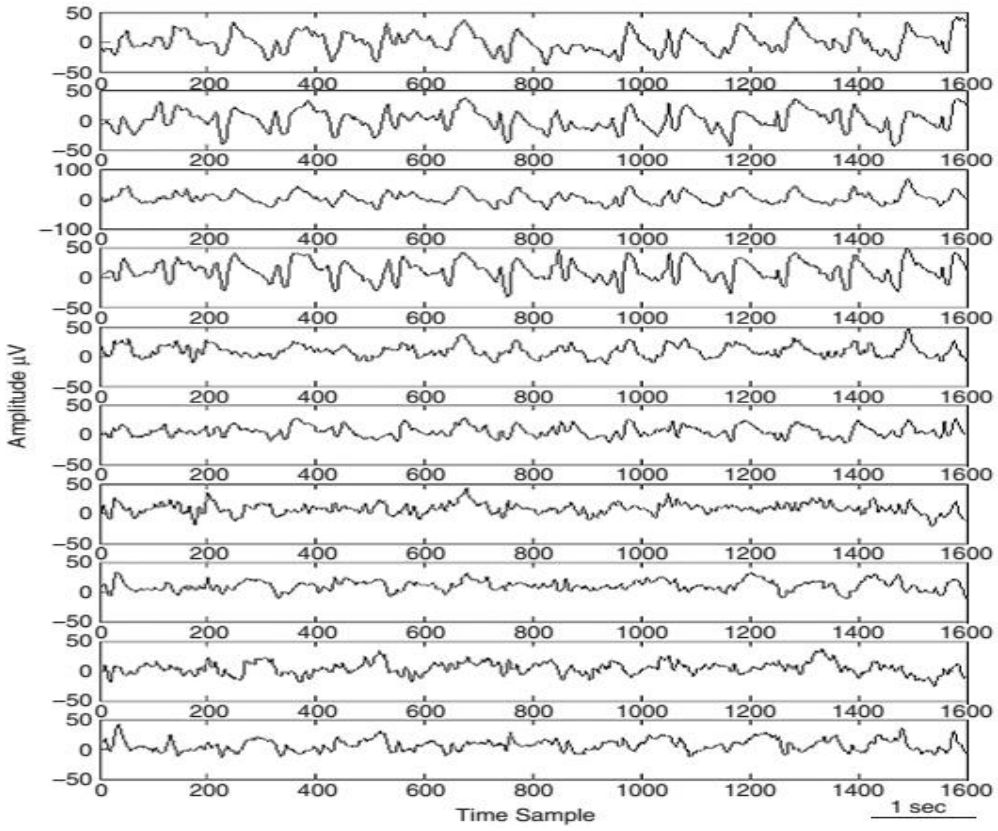

Figure: 1.7 EEG recording of a normal adult

Notch filters with a null frequency of 50 Hz are often necessary to ensure perfect rejection of the strong 50 Hz power supply. In this case the sampling frequency can be as low as twice the bandwidth commonly used by most EEG systems. The commonly used sampling frequencies for

EEG recordings are 100, 250, 500, 1000, and 2000 samples/s. The main artefacts can be divided into patient-related (physiological) and system artefacts. The patient-related or internal artefacts are body movement-related, EMG, ECG (and pulsation), EOG, ballistocardiogram, and sweating. The system artefacts are 50/60 Hz power supply interference, impedance fluctuation, cable defects, electrical noise from the electronic components, and unbalanced impedances of the electrodes. Often in the preprocessing stage these artifacts are mitigated and the informative information is restored.

1.3 Artifacts in EEG

1. Muscle Activity

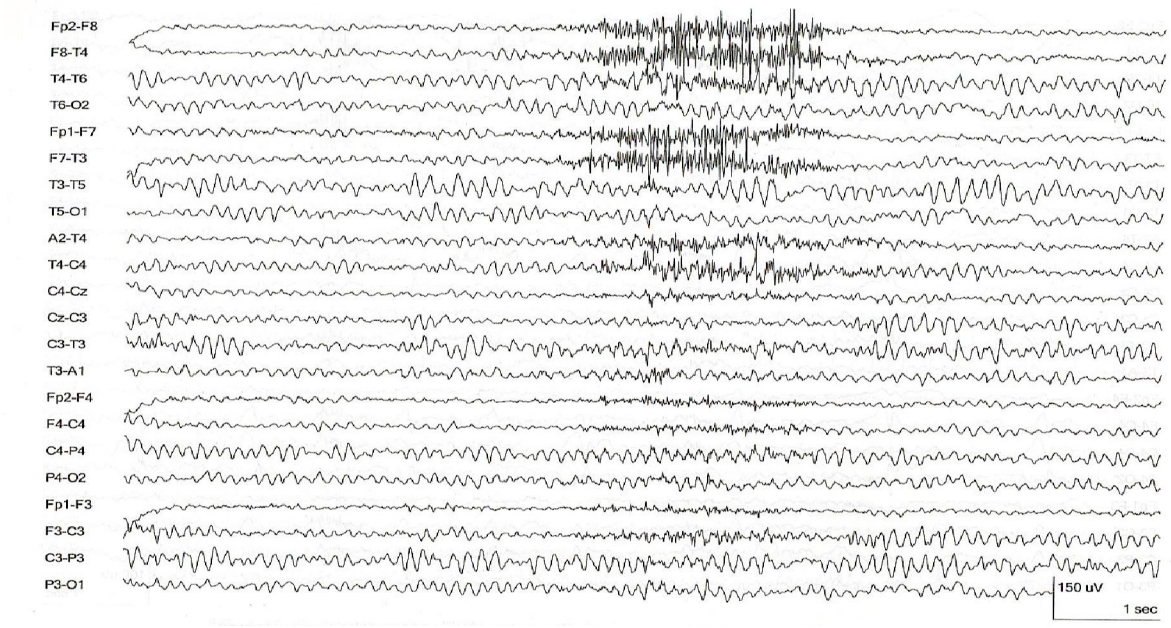

Figure: 1.8 EMG artifacts in EEG

The most common artifacts are myogenic potentials. The most common causes are Frontalis and Temporalis muscles (clenching of jaw muscles). The duration of generated potentials in the muscles are generally shorter than the duration of the generated potentials in the brain. On the basis of duration, morphology and the rate of firing (i.e frequency), they can be identified easily.In some movements disorder, particular pattern of of electromyogram (EMG) artifacts can

occur. Production of rhythmic 4-to-6 hz sinusoidal artifacts by Essential Tremor and Parkinson Disease may mimic cerebral activity.

Hemifacial Spasm is yet another disorder that can produce repetitive muscle artifacts. During intermittent photic stimulation, a special type of EMG artifact, Photomyoclonic response, occurs. Frontalis and orbicularis muscles are contracted by some subjects. Approximately, 50-60 milliseconds after each flash, these contractions occur and after eye-opening, they dissapear, and use of paralyzers, are located mostly frontally, and have no concomitant EEG changes.

2. GLOSSOKINETIC ARTIFACT

The tongue (like the eyeball) functions as the dipole, with tip negative with respect to the base in addition to muscle activity. As it is more mobile, in this case, the tip of the tongue is the most important part. The production of artifacts by the tongue as broad potential fields that drops from Frontal to Occipital areas. They are less steep than the production of artifacts by eye-movements. The amplitude of potential is inferiorly greater than in the regions of parasagittal. The frequency is variable but usually in the delta range and synchronously occurs when the patient says "lah-lah-lah-lah" or "lilt-lilt-lilt-lilt", which can be verified by our technologist. Similar artifacts can be produced by chewing and sucking, which are observed among young patients. However, dementia patients and the patients who are uncooperative, can also be observed with these similar artifacts.

3. EYE MOVEMENTS

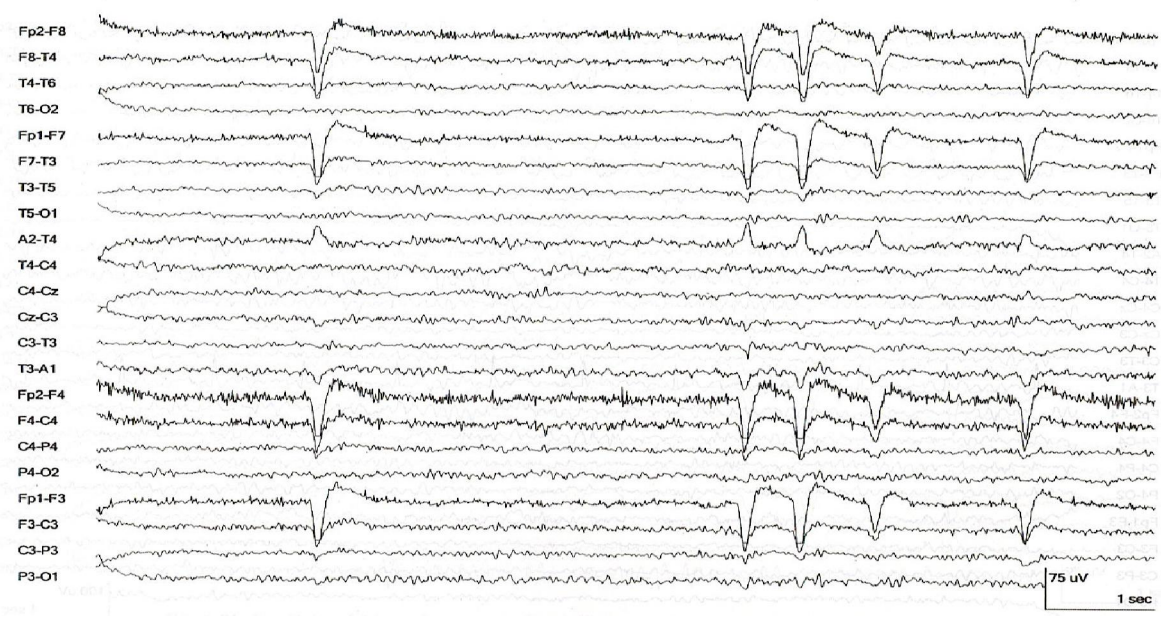

Figure: 1.9 ocular artifacts in EEG

On all EEGs, eye movements are observed and are useful in identifying sleep stages.The eyball acts as a dipole with antiriorly oriented positive pole (cornea) and posteriorly oriented negative pole (retina). A large-amplitude alternate field current is generated, when the globe rotates about its axis, which id detectable by any electrode near the eye. The artifacts from other sources comes from EMG potentials from muscles in and around the orbit.

A blink is a means to observe vertical eye movements. A positive pole (i.e. cornea) is moved closer by a Frontpolar (Fp1-Fp2) electrodes with a blink and that produces symmetric downward deflections. The positive pole (i.e cornea) of the globe moves away from the Frontpolar electrode, during a downward eye movement, that produces an upward deflection best recorded in channel 1 to channel 5 in the bipolar longitudinal montage.

Lateral Frontal electrode (F7 and F8; see images below) is mostly affected by lateral eye movement. The positive poles from the globe moves towards F7 and away from F8. The maximum positivity in electrode F7 and maximum negativity in electrode F8 is recorded using a bipolar longitudinal montage, and artifacts do not occur in channel 9 and 13 or 10 and 14. In electrode F7, there may be present a so-called rectus lateralis. It is observed best in vertex reference montage. The opposite occurs with right lateral eye movement.

4. **ECG artifacts:**

Over the surface of the scalp, some individual variation in the amount and persistence in ECG artifacts are related to the field of heart potentials. People with short and wide necks generally have the largest ECG artifacts on their EEGs. Consequently, the voltage and apparent surface of the artifact vary from derivation to derivation and from montage to montage. Using earlobe electrodes A1 and A2, the artifacts is best observed best in referential montages.

ECG artifact is recognized easily by its rhythmicity and coincidence with ECG tracing (each "sharp wave" equals artifact that synchronizes with each QRS complex of the ECG channel). The situation becomes difficult when cerebral abnormal activity (eg, sharp waves) appears intermix ed with EEG artifact, and the former may be overlooked. The EEG technologist should apply electrodes routinely to record ECG.

Figure: 1.10 ECG artifacts observed in EEG

5. PULSE

When an EEG electrode is placed over a pulsating vessel, pulse artifact occurs. The pulsation causes slow waves that stimulates EEG activity. There is a direct relationship between ECG and pulse waves. The QRS complex (i.e. electrical component of the heart contraction) happens slightly ahead of the pulse waves.

6. RESPIRATION ARTIFACTS

Two kind of artifacts are produced by respiration. The first kind is in the form of slow and rhythmic activity, that ae synchronous with the body movements of respiration and affects the impedance of one electrode. The other kind can be slow or sharp that occur with inhalation or exhalation synchronously and involves electrodes on which the patient is lies. To monitor respiration, several commercially available devices can be coupled to the EEG machine. One channel can be dedicated to respiratory movements as with the ECG. To monitor respiration by the EEG technician making notations with a pencil, is the simplest way.

Out of all above artifacts the most obvious and influencing artifact is ocular artifact and it is challenging to remove it because its frequency band overlaps with EEG signal. There are several methods to handle with ocular artifacts, some of them we have discussed in chapter 2 and proposed a method in chapter 3. Chapter 4 will talk about results and in chapter 5 we have given our conclusion.

Chapter 2 : Literature review:-

To analyze EEG accurately it is necessary to remove artifacts from EEG which gets coupled with signal at the time of recording and can't be eliminated at preprocessing stage. As we have discussed in chapter 1 ocular artifact is most obvious artifact in EEG signal, to deal with ocular artifacts very much of research has been done and still going on. The main algorithms to deal with ocular artifacts are

1. ocular artifacts removal using DWT
2. ocular artifact removal using stationary wavelet transform
3. ocular artifact removal using independent component analysis
4. ocular artifact removal using wavelet enhanced ICA

2.1 Ocular artifacts removal using DWT:-

1. Algorithm steps:-

1. Calculate DWT of raw EEG signal up to 4 level of decomposition.
2. Calculate threshold for coefficients of level 3 and level 4.
3. Apply hard or soft thresholding at level 3 and level 4 coefficients.
4. Reconstruct noise free signal using modified wavelet coefficients.

In Estreda et al [19] has presented method for denoising of EEG signal using DWT thresholding technique.

2. Discrete Wavelet Transform:-

To understand the importance of wavelet transform, we need to understand drawbacks of Fourier transform (FT), FT has mainly to drawbacks:

1. When we transform signal from time domain to frequency domain, we lose the time information regarding the signal.
2. The frequency resolution is fixed, i.e. we get coefficients at nw_0 points in frequency domain.

To get rid of these drawbacks was the motivation of Short Time Fourier Transform (STFT), STFT is obtained by calculating signal for short time duration using some window. The window

is traversed through entire time duration and FT is calculated for windowed signal. STFT can be computed as:

$$STFT\big(f(w,s)\big) = \int g^*(t-s)f(t)e^{-jwt}dt$$

Where g(t-s) is the window used to obtain short duration signal.

Based on STFT continuous wavelet transform (CWT) is defined, it is different from STFT because of scaling windows. CWT is calculated as,

$$CWT\big(f(a,b)\big) = \int f(t)\psi_{a,b}(t)dt$$

$$\psi_{a,b}(t) = \frac{1}{\sqrt{a}}\psi\left(\frac{t-b}{a}\right), a \in \mathbb{R}^+, b \in \mathbb{R}$$

Here $\psi_{a,b}(t)$, are the wavelet window functions and are derived from mother wavelet. "a" and "b" are scaling parameter and location parameter respectively. There are several mother wavelets to do wavelet transform analysis like, Haar, symlet, daubechies etc.[20]

DWT is discrete transform of CWT, i.e. by using discrete values of "a" and "b" CWT calculation becomes DWT. DWT can be calculated as,

$$DWT_{m,n}(f) = {a_0}^{-m/2}\int f(t)\psi({a_0}^{-m_t} - nb_0)dt$$

Here a_0 and b_0 are set to be 2 and 1, respectively, the DWT is the output obtained from two QMF (quadratic mirror function), high pass FIR filter is "g" and low pass FIR filter is "h".

$$g(n) = (-1)^n h(1-n)$$

Here the low pass filter h is associated with scaling function, whereas the high pass filter g is associated with the mother wavelet.

$$\phi(x) = \sum_n h(n)\sqrt{2}\,\phi(2x-n)$$

$$\psi(x) = \sum_n g(h)\sqrt{2}\,\phi(2x-n)$$

Thus the outputs of QMF are characterized as:

$$\overline{H}_L = \sum_n h(n-2L)x(n)$$

$$G_L = \sum_n g(n-2L)x(n)$$

From above equations we can say that the signal x(n) is passed through filters h(n-2L) and g(n-2L) which are low pass and high pass filter respectively, this transforms the actual signal into two frequency subbands: [0-W_n/2] and [W_n/2-W_n]. The output of low pass filter H_L is called approximation components and it contains low resolution components. The output of high pass filter G_L is called detailed components and it represents the high resolution components. The DWT tree structure is constructed by recursively applying the decomposition process on approximation components. In figure (2.1) the decomposition tree structure is shown where H_0 is

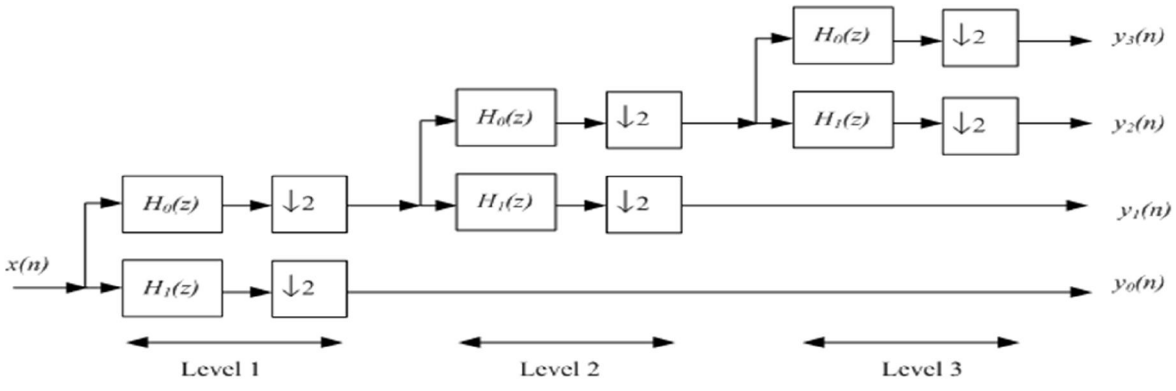

Figure: 2.1 DWT decomposition tree

Low pass filter and H_1 is high pass filter. At each level of decomposition after passing the signal through filters, it is decimated by a factor 2, means time resolution decreases at each level of decomposition. But frequency resolution is increased at each level.

The reconstruction process follows the inverse procedure and signal is reconstructed without any loss of information. The reconstruction process is called inverse discrete wavelet transform (IDWT) and it is different from DWT in the order where it uses up-sampling and filtering at the place of filtering and down-sampling. In following figure the reconstruction filter bank is shown,

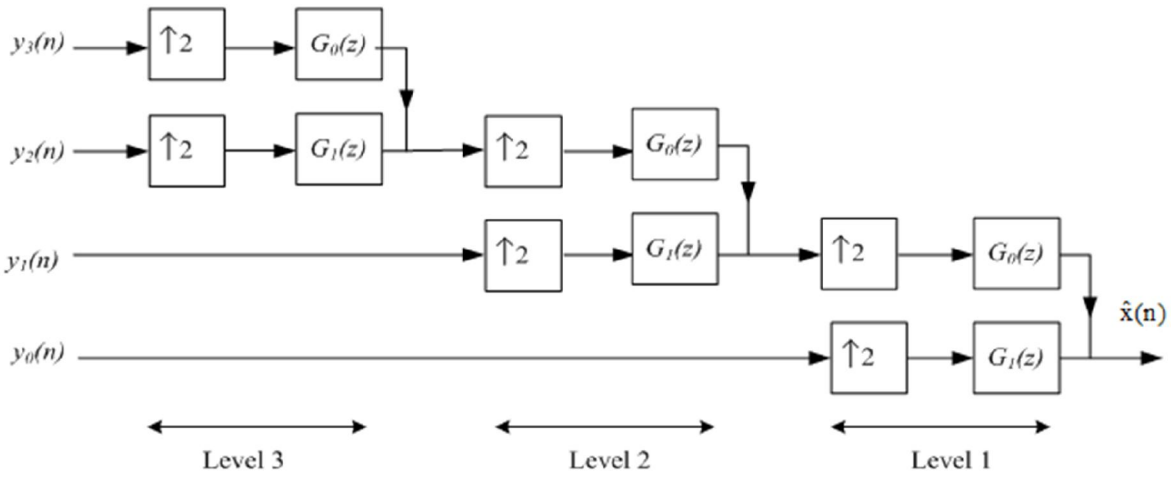

Figure: 2.2 DWT reconstruction tree

Here G_0 is the QMF of H_0 and G_1 is the QMF of H_1. At each level after passing the signal through filters it is up-sampled by 2.

3. Thresholding:

Denoising is the process of removing artifacts from raw signal. After calculating DWT of raw signal a predefined threshold is calculated. Since ocular artifacts has significant components in 0-16 Hz, thresholding will be done only those subbands lying in the frequency region of 0-16 Hz. Generally four level of decomposition is done using DWT and threshold is applied on 3rd and 4th level coefficients.

The threshold value is selected using universal threshold value as suggested in [21] and can be estimated as,

$$T_j(0) = \sqrt{2\,\sigma^2 \log(d)}$$

Where j is level of decomposition, T is threshold value, N is no. of components at j^{th} kevel and σ^2 is noise variance. The noise variance can be calculated by using MAD (median absolute deviation) and it is given by [22],

$$\sigma^2 = \frac{median(|W_j|)}{0.6745}$$

where W_j is detailed components at j^{th} level of decomposition.

The widely used thresholding techniques are soft thresholding and hard thresholding.

Hard thresholding rule can be defined as,

$$d_k^{\wedge l} \begin{cases} 0 & |d_k^{\wedge l}| < \lambda \\ d_k^{\wedge l} & |d_k^{\wedge l}| \geq \lambda \end{cases}$$

Where, $d_k^{\wedge l}$ is detailed coefficient at lth level and λ is the universal threshold value.

Soft thresholding rule can be defined as,

$$d_k^{\wedge l} \begin{cases} 0 & |d_k^{\wedge l}| < \lambda \\ sgn(d_k^{\wedge l})(d_k^{\wedge l}) & |d_k^{\wedge l}| \geq \lambda \end{cases}$$

Where, $d_k^{\wedge l}$ is detailed coefficient at lth level and λ is the universal threshold value.

In case of ocular noise hard thresholding is preferred over soft thresholding because ocular artifact occurs for short time duration and soft thresholding modifies entire signal.

2.2 Ocular artefact removal using SWT

In Krishnaveni et al [23] has proposed a method to remove ocular artifacts using stationary wavelet transform (SWT) and adaptive thresholding. This method follows steps as shown in figure,

1. Algorithm steps:

1. SWT is applied to expand contaminated signal.

2. Optimal threshold is selected for 3rd to 6th level of decomposition on minimum risk value and

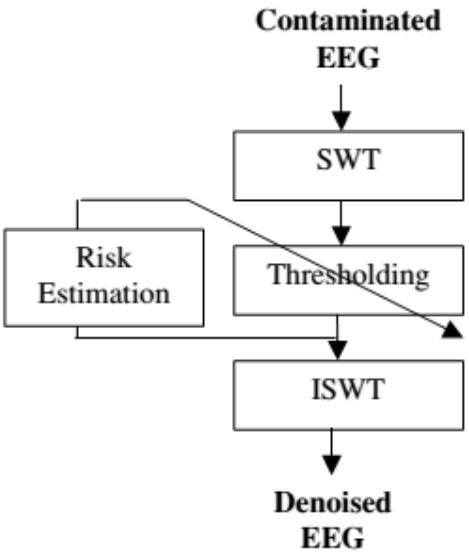

Figure: 2.3 basic adaptive denoising procedure

Soft-like thresholding is applied for optimal noise removal.

3. Inverse wavelet transform is applied applied on thresholded wavelet components and noise free signal is obtained.

2. Stationary wavelet transform:

SWT is calculated same as DWT only downsampling and upsampling blocks are not present, this can be noticed from SWT filter bank figure,

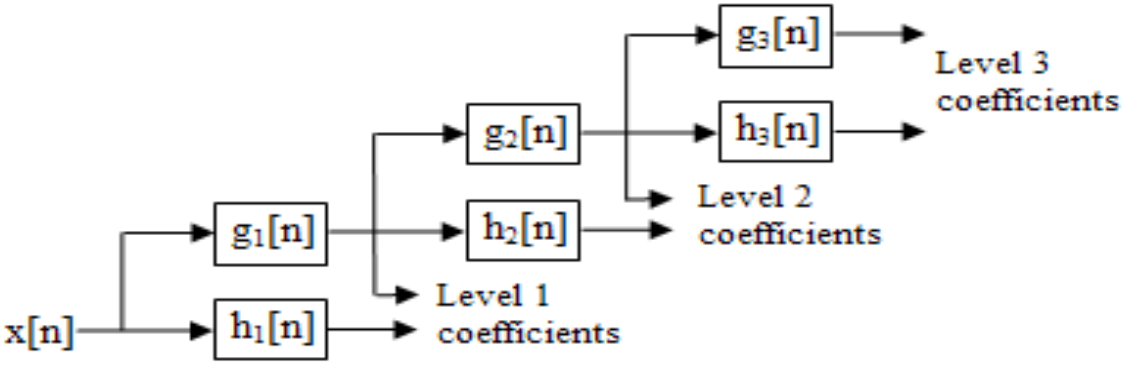

Figure: 2.4 SWT decomposition tree

In figure we can see the difference between DWT and SWT, there is no downsampler after filters. SWT is used because of its time invariance property, since there is no downsampling no time information is lost and hence it produces smoother results in low frequency bands. SWT also gives approximation and detailed components at each level but at each level no. of components will be same.

3. Thresholding:

The initial threshold value is universal threshold value same as discussed in DWT based denoising method,

$$T_j(0) = \sqrt{2\,\sigma^2 \log(d)}$$

Where j is level of decomposition, T is threshold value, N is no. of components at j^{th} kevel and σ^2 is noise variance. The noise variance can be calculated by using MAD (median absolute deviation) and it is given by [24],

$$\sigma^2 = \frac{median(|W_j|)}{0.6745}$$

where W_j is detailed components at j^{th} level of decomposition.

Since soft thresholding functions have discontinuous derivatives they cannot be used for adaptive thresholding as we require continuous derivative for minimum condition criteria calculation. Hence authors used a soft-like thresholding and is defined as,

$$\eta_k(y^j\,i, t) = \begin{cases} y^j\,i + t - \dfrac{t}{2k+1}, & y^j\,i < -t \\ \dfrac{1}{(2k+1)t^{2k}} \cdot (y^j\,i)^{(2k+1)}, & |y^j\,i| \le t \\ y^j\,i - t + \dfrac{t}{2k+1}, & y^j\,i > t \end{cases}$$

Where k is a positive integer, $y^j\,i$ is detailed coefficients at j^{th} level and t is threshold value.

Conditions given by krishnaveni et al [23] are used to find optimal threshold using soft-like threshold and using the optimal threshold noisy part is suppressed in noisy signal. Once the thresholding is done inverse wavelet transform is applied.

2.3 Ocular artefact removal using ICA

In [25] the method suggested for ocular artifact removal is blind source separation using independent component analysis and then zeroing the artifactual components.

1. Algorithm steps:

1. Estimate independent components and mixing matrix using ICA.
2. Identify the artifactual sources using some IC marker.
3. Zero the column corresponding to artifactual independent components.
4. Mix the estimated sources by multiplying them with modified estimated mixing matrix.

2. Independent component analysis:

The basic concept of ICA is in fact that signals can be separated into their actual independent sources. This concept is applicable at places where mixed components can be assumed to be independent of each other and is very useful in denoising of signals.

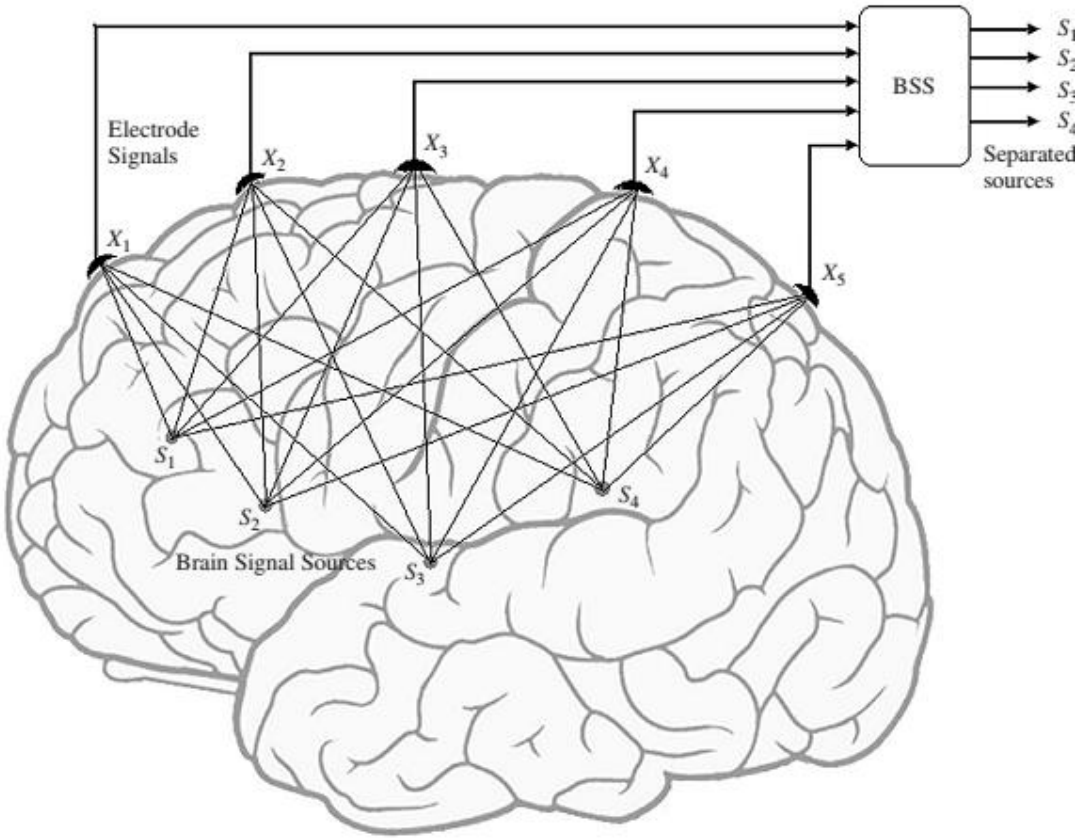

Figure: 2.5 BSS concept; mixing and blind separation of EEG signal.

BSS is used to find the independent components or sources from mixed signal, i.e. only information available is mixture of several independent sources at several recording channels.

To apply ICA on EEG signals some assumptions are made:

1. The cerebral signal and artifact signal are linearly combined and are statistically independent.
2. The number of recording channel must be greater or equal to number of independent sources.
3. The delay because of propagation through mixing medium are insignificant.

Mathematically we can express the linear ICA model as,

$$X = A \times S$$

Where X is mixed signal recorded through different channels, A is unknown mixing matrix [26]. ICA estimates demixing matrix W such that the estimated independent sources U are very close to actual sources S.

$$u = W \times X \approx S; \quad W = A^{-1}$$

Once the independent components are calculated artifactual sources are identified using some IC marker (some parameter which discriminates artifactual and EEG sources) and the column corresponding to those sources are made zero in estimated mixing matrix. The sources are mixed again by multiplying modified estimated mixing matrix with estimated sources.

In Castellanos et al [27] method for automatic noise removal of ocular artifact using wavelet enhanced ICA is proposed and the steps taken are as follow:

1. Estimate independent components and mixing matrix using extended infomax ICA.
2. The artifactual sources are manually identified.
3. Apply DWT on artifactual source.
4. Apply thresholding and reconstruct the artifactual source.
5. Estimate the mixed signal by multiplying independent components with estimated mixing matrix.

Chapter 3 : Proposed Method

We have discussed four methods for ocular artifacts removal in previous chapter, Krishnaveni et al [23] proposed a method of adaptive thresholding which gives good results in ocular artifact suppression but it also suppresses EEG signal, due to which we lose information. Cstellanos et al [27] discussed a wavelet enhanced ICA in which artifactual independent component detection is manual.

3.1 Motivation:

We wanted to use an automatic wavelet enhanced ICA (wICA), which is suggested by Mahajan et al [29]. In this method kurtosis and mMSE are used as IC marker to identify artifactual independent component detection

3.2 Methods:

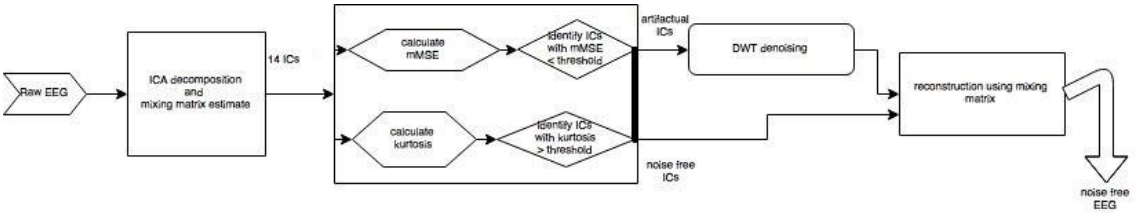

Figure: 2.6 Block diagram of the proposed eye blink artifact removing algorithm

1. **Independent component analysis:**

As discussed in previous chapter ICA is a statistical tool to separate mixed recordings from several channels into independent sources. Suppose that an array of channels to provide N observed signal

$$x(k) = [x_1(k), x_2(k), \ldots., x_N(k)]^T$$

And the actual sources are

$$s(k) = [s_1(k), s_2(k), \ldots., s_N(k)]^T$$

Here the assumptions are that the sources have non Gaussian distribution and they are mutually statistically independent. The main purpose of ICA is to estimate a demixing matrix W such that

$$s = W \times x$$

W defines that the transformed occurred in such a way that the mutual information is minimized among all independent sources. Mutual information measures the information dependency between two random variables. So many algorithms are designed to perform ICA, we have chosen infomax ICA. According to Bell et al [33] it is an unsupervised technique which uses information maximization in a single layer neural network (feed forward) and gives nonlinear outputs. For sources having super-Guassian distribution this technique is efficient.

2. **Discrete wavelet transform:**

The theory of wavelet transform has been discussed in previous chapter. We apply four level of decomposition on artifactual components. The 3rd and 4th levels of coefficients are thresholded using hard threshold technique. 3rd and 4th levels of decomposition are chosen because they lie in the frequency range 0-16 Hz.

3.3 Modified multiscale sample entropy (mMSE):-

Entropy is the measure of randomness, means more the signal is random in nature more is the value of entropy, EEG signal is very random in nature whereas eye-blinks occur for very small duration and with higher probability, hence the entropy value of ocular signal will be less compared EEG signal. According to above argument entropy can be used as IC marker to identify the artifactual independent component. In Bose et al [28] it is revealed that MSE gives better information regarding EEG than other existing entropy. The mMSE is calculated by initially coarse graining of each independent component for multiple scale, then sample entropy of each scale is calculated. The coarse graining of IC can be mathematically given as,

$$y_j^{(\tau)} = \frac{1}{\tau} \sum_{i=(j-1)\tau+1}^{j\tau} u_i; \;\; 1 \le j \le {}^{N}/_{\tau}$$

Where y is coarse grained sequence at scale factor TAU. ‘u’ is the IC time sequence and N is length of each IC. The MSE for each grained independent component can be calculated as [29]

$$nMSE(m,r) = log\left(\frac{{B_r}^m}{{A_r}^m}\right)$$

Where m = 2 and r = 0.2 * SD, standard deviation of data sequence.

Kurtosis:-

It is a fourth-order statistical parameter to study the peaked distribution of any random variables, it can be mathematically calculated as,

$$k = m_4 - 3m_2^2$$

$$m_n = E\{(x - m_1)^n\}$$

Here m_n, m_1 and E are n^{th} order moments of the random variable, mean and expectation function, respectively [30]. The signals with peak distribution will have higher values of kurtosis, hence ocular signals will have higher values of kurtosis than EEG signals. With support of above argument kurtosis can be used as IC marker.

Threshold value selection:-

The criteria for threshold selection is discussed in Mahajan et al [29]. Threshold value for mMSE can be mathematically given as,

$$Lower\ limit = \bar{x} - \frac{s}{\sqrt{N}} \times t_{N-1}$$

Threshold value for kurtosis is calculated by,

$$Upper\ limit = \bar{x} + \frac{s}{\sqrt{N}} \times t_{N-1}$$

Where, $\bar{x}$ is sample mean, s is sample standard deviation, N no. of ICs and $t_{N-1} = 2.201$. ICs having mMSE values less than lower limit or kurtosis value above upper limit are considered as artifactual components.

On each artifactual source DWT denoising method discussed at the beginning of this chapter is applied, now the modified independent sources are used to calculate mixed signal using estimated mixing matrix.

3.4 Steps of proposed algorithm:

1. Estimate independent sources and mixing matrix using infomax ICA.
2. Calculate mMSE and kurtosis.
3. Select artifactual component using mMSE and kurtosis information.
4. Apply discrete wavelet transform on each artifactual source.
5. Apply the hard thresholding technique.
6. Estimate the mixed signal using modified ICs and estimated mixing matrix.

Chapter 4 : Results and Discussions

The 32 channel preprocessed EEG signals is taken from www.physionet.org , first 14 channels of 10s are used in our experiment and are plotted using MATLAB in fig 4.1.

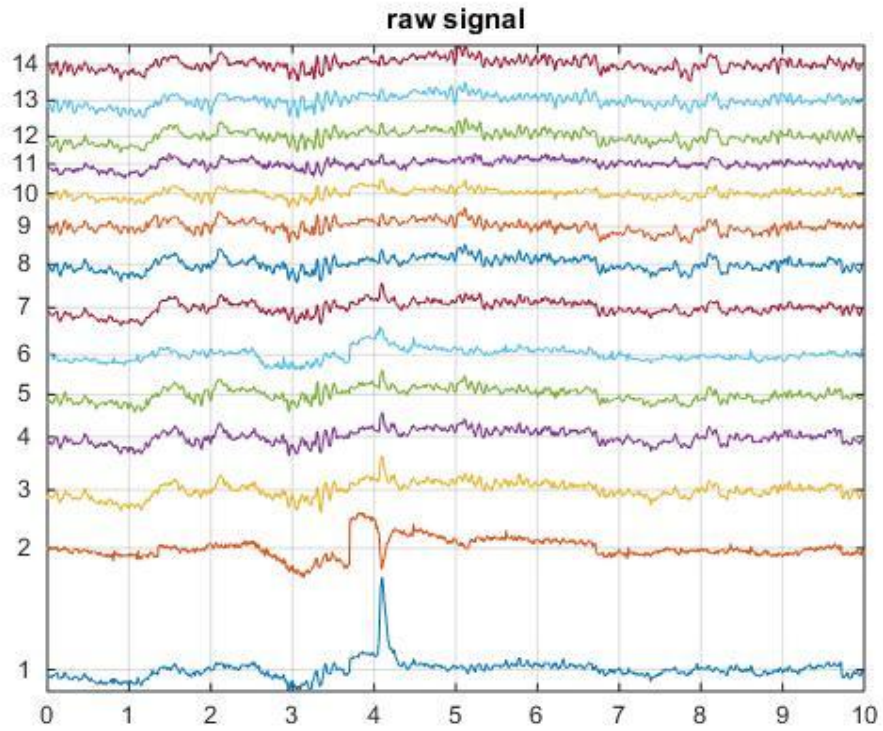

Figure: 4.1 Raw EEG signal

From fig 4.1 it is clearly visible that channel 1 is severely affected by ocular artifact around time instant 4s. After the decomposition of raw signal using Infomax ICA, 14 independent components are obtained are shown in fig 4.2. Then using mMSE and kurtosis, the ocular artifact related independent components are identified, then stationary wavelet transform and novel thresholding technique are applied to suppress noise. The mMSE plot for each channel is shown in fig 4.3, we can notice from the plot that channel 2, 5 and 8 are the components affected by ocular artifact. In support of mMSE one more statistical parameter kurtosis is calculated and shown in fig 4.4. Kurtosis supports that 5^{th} independent component is severely affected by ocular artifact. In fig 4.5 and fig 4.6 we have shown the ICs before and after thresholding and it is clearly visible the peak part in 5^{th} IC is completely suppressed. The final reconstructed noise free signal is shown in fig 4.7. It can be easily observed from fig 4.7 that ocular artifact has been efficiently removed from channel 1 while keeping the rest signal unfazed.

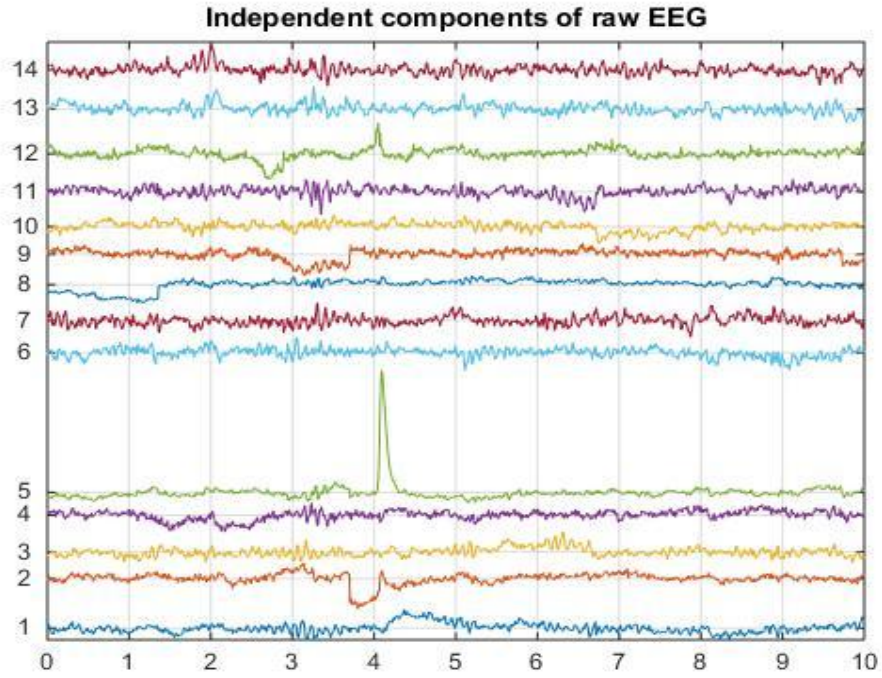

Figure: 4.2 independent components of raw EEG

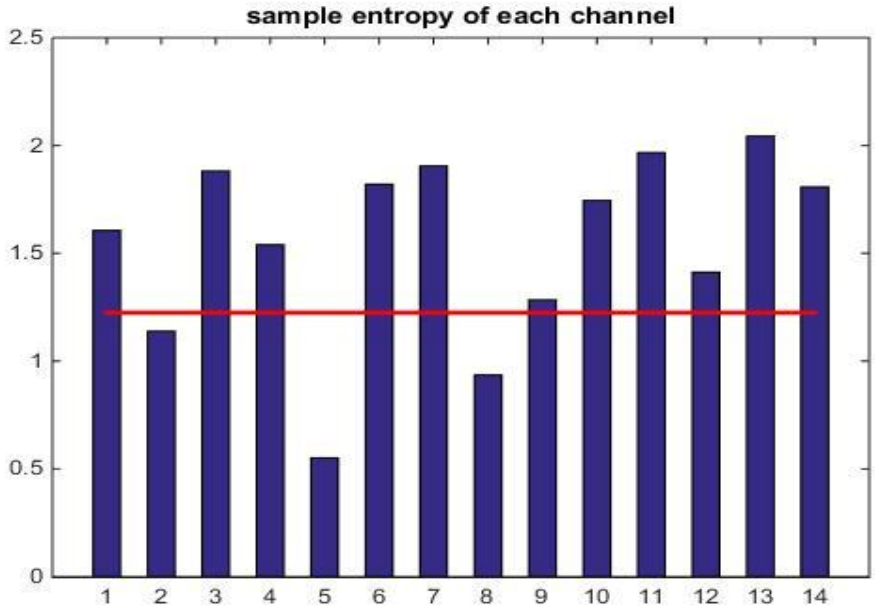

Figure 4.3 mMSE plot for each channel.

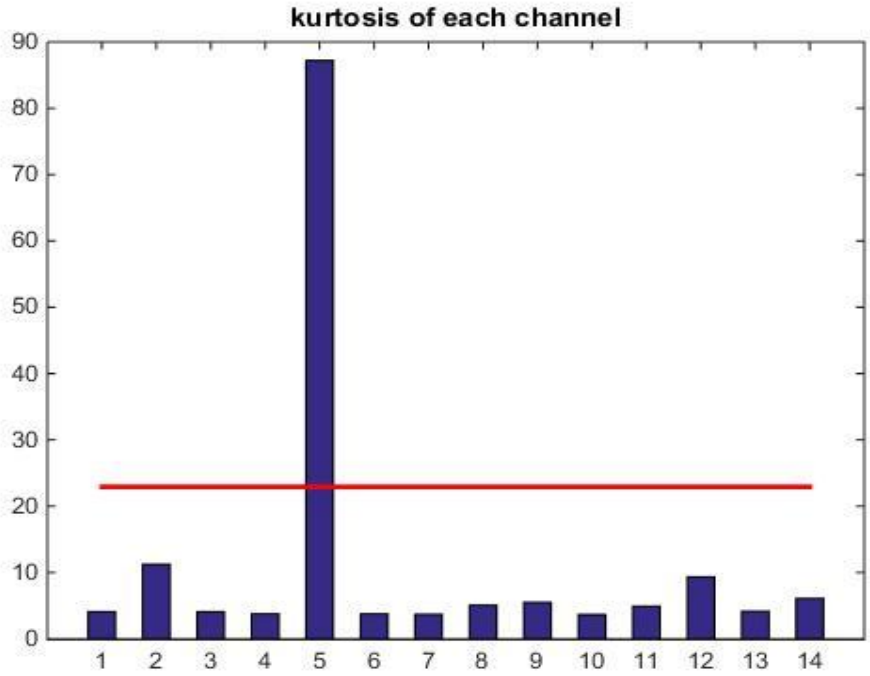

Figure 4.4 kurtosis of each independent component.

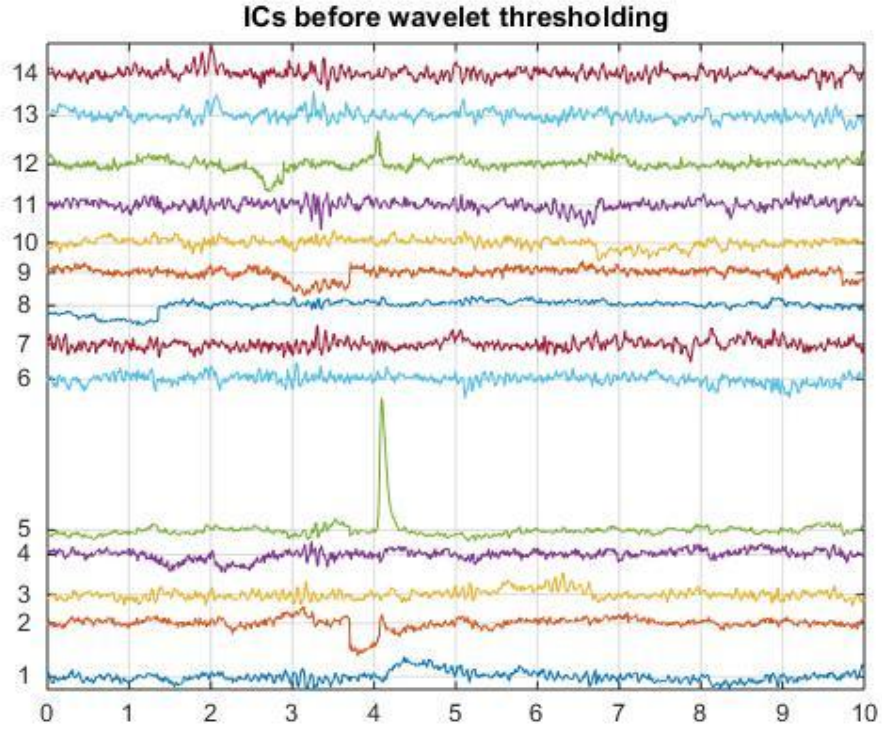

Figure: 4.5 ICs before thresholding

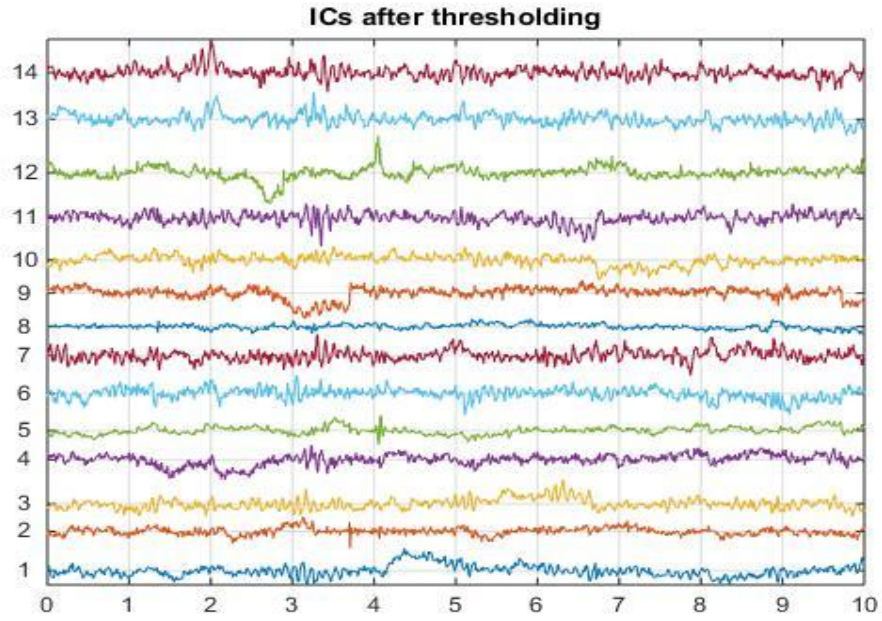

Figure: 4.6 ICs after thresholding

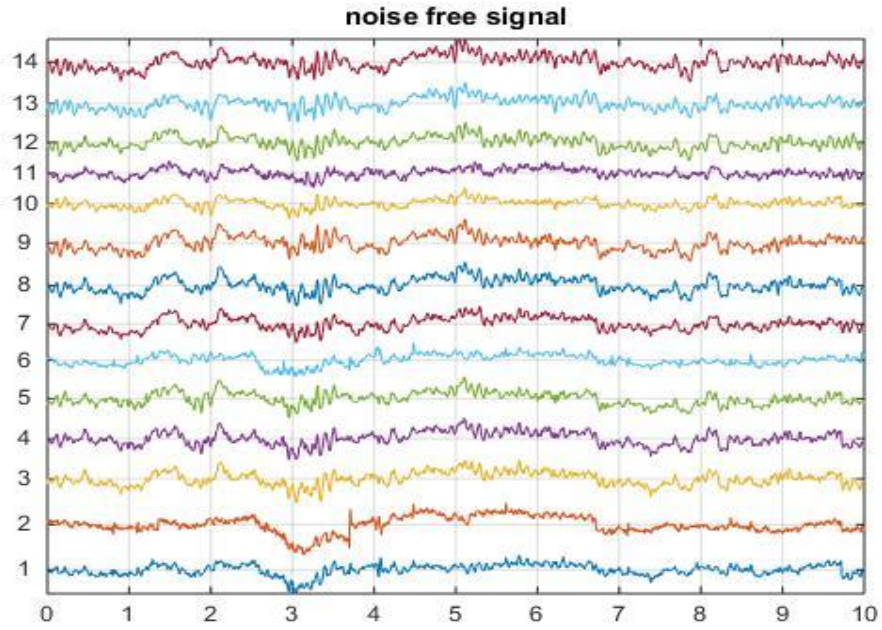

Figure: 4.7 Reconstructed noise free signal

To measure the performance of our proposed technique we compared the result with zeroing ICA technique in terms of correlation, mutual information and coherence.

4.1 Correlation:

Correlation is used to measure the linear relationship between to random variables, it used second order statistics to find the measure of similarity, the maximum value of correlation between two signal can be '1'. It can be mathematically given as,

$$r_{xs} = \frac{cov(x,s)}{\sigma_x \sigma_s}$$

Here x is the raw EEG signal and s is the noise free EEG signal, σ is the standard deviation and cov is the covariance of two random variable x and s. the comparison among three methods in term of correlation is given in table 4.1.

Electrode no.	Zeroing ICA	wICA
1	0.44436389	0.58350784
2	0.70345467	0.79362655
3	0.78095615	0.83155793
4	0.86903185	0.89574039
5	0.82431334	0.86538911
6	0.74197018	0.81504935
7	0.78898317	0.84224212
8	0.93829525	0.95204139
9	0.83382118	0.85651022
10	0.79313588	0.84879678
11	0.86821270	0.88574868
12	0.87662739	0.90155125
13	0.87989676	0.91064858

14	0.92177272	0.93717438

Table: 4.1 Correlation table

4.2 Mutual information:

Mutual information is a measure of amount of information noise free EEG contains about raw EEG signal, it is a non-parametric method and estimates the relevance of two random variables. According to Shannon information theory MI can be calculated by Kullback-Leibler distance between the product of the marginal pdfs of random variable x and y and their joint pdf, which can be given as,

$$I(x,y) = \int_{-\infty}^{\infty}\int_{-\infty}^{\infty} f(x,y)\log\left(\frac{f(x,y)}{f(x)f(y)}\right)dxdy$$

If two random variables are closely related they will have large number of mutual information. In table 4.2 three methods are compared in terms of mutual information.

Electrode no.	Zeroing ICA	wICA
1	0.304379980163526	0.421345989714540
2	0.496722419919256	0.919198554761350
3	0.499119718783075	0.624192787584858
4	0.691544735371566	0.702270443395462
5	0.640776426268665	0.731535547749328
6	0.581536130867213	0.605759727591838
7	0.600084518134429	0.712348044253540
8	0.976926047997557	1.19898931659061
9	0.613492684716348	0.952877474544051
10	0.571230229333005	0.749866703094726
11	0.734403024728324	0.818754361349984

12	0.724593256594467	0.900956502541267
13	0.809041230242952	0.977230629514682
14	0.976560159447905	1.27058940764471

Table: 4.1 Mutual information table

4.3 Coherence:

To analyze the performance in frequency domain coherence is measured between raw EEG data and noise free EEG data. It is calculated in magnitude square term. For all three method coherence is plotted in figure 4.7, 4.8 and 4.9.

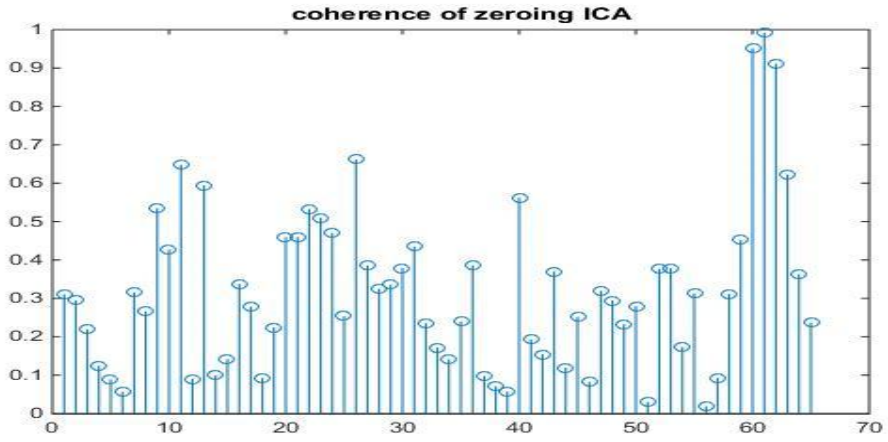

Figure: 4.7 coherence of zeroing ICA

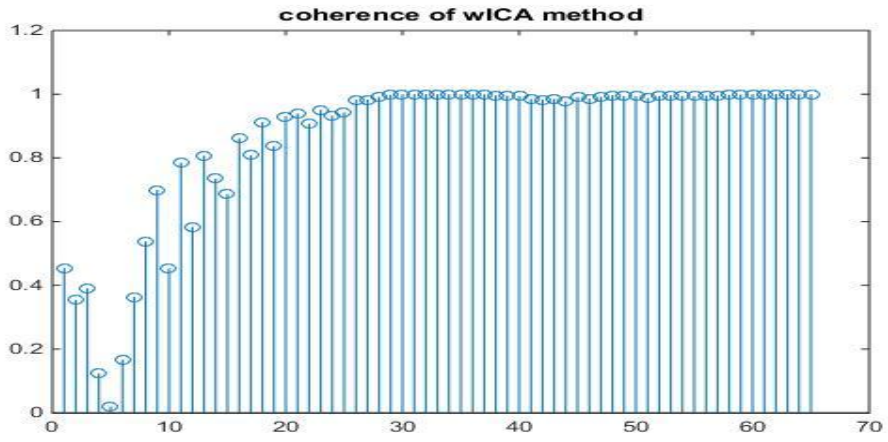

Figure: 4.8 coherence of wICA

Chapter 5 : Conclusion

In this work we have presented a new approach towards wavelet enhanced ICA, we have used mMSE and kurtosis to detect the artifactual components automatically, Mahajan et al [28] displayed their performance in terms of sensitivity (90%) and specificity (98%), nMSE is good at recognizing EEG patterns because of its randomness and kurtosis is good at recognizing peaked signal because they have high kurtosis values. We compared our result with ICA based method zeroing ICA in terms of correlation, mutual information and coherence. Our result is far superior to it in all three terms, in correlation measure our method not only gives better results for unaffected recording channel but it improves the result from 0.44 to 0.58 for most affected recording channel, which means our method only suppresses the noise without introducing additional noise. When we compare the results in terms of mutual information it improves from 0.30 to 0.42 for most affected recording channel. When we study the coherence graph we notice that the wICA method is affecting those frequencies too which are not present in ocular artifacts frequency range but our method has only affected the frequency range 0-16 Hz which is ocular artifact's frequency band. We can extend this work by using different mother wavelets to best approximate eye blink and other ocular artifacts.

References

[1] Caton, R., 'The electric currents of the brain', Br.Med.J., 2, 1875, 278.

[2] Walter, W. G., 'Slow potential waves in the human brain associated with expectancy, attention and decision',Arch. Psychiat. Nervenkr., 206, 1964, 309–322.

[3] Shipton, H. W., 'EEG analysis: a history and prospectus',Annual Rev., Univ. of Iowa, USA, 1975, 1–15.

[4] Fischer, M. H., 'Elektrobiologische Auswirkungen von Krampfgiften am Zentralnervensystem', Med.Klin., 29, 1933, 15–19.

[5] Fischer, M. H., and Lowenbach, H., 'Aktionsstrome des Zentralnervensystems unter der Einwirkung von Krampfgiften, 1. Mitteilung Strychnin und Pikrotoxin'Arch. F. Exp. Pathol.und Pharmakol., 174, 1934,357–382.

[6] Kornmuller, A. E., 'Der Mechanismus des Epileptischen Anfalles auf Grund Bioelektrischer Untersuchungen am Zentralnervensystem',Fortschr. Neurol. Psychiatry, 7, 1935, 391–400; 414–432.

[7] Caspers, H., Speckmann E.-J., and Lehmenk¨ uhler, A., 'DC potentials of the cerebral cortex, seizure activity and changes in gas pressures', Rev. Physiol., Biochem. Pharmacol., 106, 1986, 127–176.

[8] Speckmann, E.-J., and Elger, C. E., 'Introduction to the neurophysiological basis of the EEG and DC potentials', inElectroencephalography Basic Principles, Clinical Applications, and Related Fields,Eds E. Niedermeyer and F. Lopes da Silva, 4th edn, Lippincott, Williams and Wilkins, Philadelphia, Pennsylvania, 1999.

[9] Shepherd, G. M.,The Synaptic Organization of the Brain, Oxford University Press, London, 1974.

[10] Caspers, H., Speckmann E.-J., and Lehmenk¨ uhler, A., 'DC potentials of the cerebral cortex, seizure activity and changes in gas pressures', Rev. Physiol., Biochem. Pharmacol., 106, 1986, 127–176.

[11] Nunez, P. L., Neocortical Dynamics and Human EEG Rhythms, Oxford University Press, New York,1995.

[12] Teplan, M., 'Fundamentals of EEG measurements',Measmt Sci. Rev., 2(2), 2002.

[13] Bickford, R. D., 'Electroencephalography', in Encyclopedia of Neuroscience, Ed. G. Adelman, Birkhauser, Cambridge (USA), 1987, 371–373.

[14] Sterman, M. B., MacDonald, L. R., and Stone, R. K., 'Biofeedback training of sensorimotor EEG in man and its effect on epilepsy',Epilepsia, 15, 1974, 395–416.

[15] Ashwal, S., and Rust, R., 'Child neurology in the 20th century',Pedia. Res., 53, 2003, 345–361.

[16] Niedermeyer, E., 'The normal EEG of the waking adult', Chapter 10, in Electroencephalography, Basic Principles, Clinical Applications, and Related Fields, Eds E. Niedermeyer and F. Lopes da Silva, 4th edn, Lippincott, Williams and Wilkins, Philadelphia, Pennsylvania, 1999, 174–188

[17] O'Leary, J. L., and Goldring, S.,Science and Epilepsy, Raven Press, New York, 1976, pp. 19–152

[18] Gotman, J., Ives, J. R., and Gloor, R., 'Automaticrecognition of interictal epileptic activity in prolonged EEG recordings',Electroencephalogr. Clin. Neurophysiol., 46, 1979, 510–520.

[19] Estrada E, Nazeran H, Sierra G, Ebrahimi F, Setarehdan SK*:* Wavelet-based EEG denoising for automatic sleep stage classification, in 21st International Conference on Electrical Communications and Computers (CONIELECOMP). *,* San Andres Cholula; 2011:295–298.

[20] Daubechies, I, "Ten Lectures on Wavelets" (CBMS-NSF Regional Conference Series in applied Mathematics), SIAM, 1992.

[21] Coifman R R and Donoho D L 1995 Translation-invariant de-noisingTechnical Report475 (Department of Statistics, Stanford University)

[22] Percival D B and Walden A 2000Wavelet Methods for Time Series Analysis (Cambridge: Cambridge University Press).

[23] V. Krishnaveni, S. Jayaraman, S. Aravind, V. Hariharasudhan, and K. Ramadoss, "Automatic identification and removal of ocular artifacts from EEG using wavelet transform," Meas. Sci. Rev., vol. 6, no. 4, pp. 45–57, 2006

[24] N. P. Castellanos and V. A. Makarov, “Recovering EEG brain signals: artifact suppression with wavelet enhanced independent component analysis,”J. Neurosci. Methods, vol. 158, pp. 300–312, 2006.

[25] D. B Keith, C. C. Hoge, R. M. Frank, and A. D. Malony, “Parallel ICA methods for EEG neuroimaging,” inProc. 20th Int. Parallel Distrib. Process. Symp., 2006, pp. 25–29.

[26] R. Mahajan and B. I. Morshed, “Sample entropy enhanced waveletICA denoising technique for eye blink artifact removal from scalp EEG dataset,” inProc. 6th Int. IEEE/EMBS Conf. Neural Eng., 2013, pp. 1394–1397.

[27] W. Bose, A. Tierney, H. T. Flusberg, and C. Nelson, “EEG complexity as a biomarker for autism spectrum disorder risk,”BMC Med., vol. 9, no. 1, pp. 1–16, 2011.

[28] H. B. Xie, W. X. He, and H. Liu, “Measuring time series regularity using nonlinear similarity-based sample entropy,” Phys. Lett. A, vol. 372, no. 48, pp. 7140–7146, 2008.

[29] M. Mamun, M. Al-Kadi, and M. Marufuzzaman, “Effectiveness of wavelet denoising on electroencephalogram signals,” J. Appl. Res. Technol., vol. 11, no. 1, pp. 156–160, 2013.